FIELD ANALYSIS OF POLYPHASE HYSTERESIS MOTOR

M. Azizur Rahman, Senior Member, IEEE
Faculty of Engineering and Applied Science
Memorial University of Newfoundland
St. John's, Newfoundland
Canada, AIB 3x5

Abstract

A comprehensive theoretical field model has been developed for hysteresis motors. Using the stator current sheet technique, the motor field equations are rigoriously derived for the air gap and hysteresis ring regions. The analysis takes into account the contribution of the reaction field of rotor magnetization to the primary air gap field due to stator current sheets alone. Unlike induction motor theory, this reaction effect represents reality in the analysis of hysteresis motor. Analytical expressions for the air gap power and rotor hysteresis power loss for the sub-synchronous mode of operation are obtained in terms of machine stator and hysteresis rotor parameters. This analysis furthermore provides a deeper insight into the sub-synchronous energy conversion process in hysteresis motors. The validity of the theory is demonstrated by comparing the experimental and theoretical results. Al though a polyphase motor is used in the analysis, the theory is applicable for single phase motors.

INTRODUCTION

In recent years the development of new and improved designs of small and medium-sized brushless synchronous motors has gained considerable momentum[1]. This is, in part, due to changing markets for synchronous ac drives and power electronics. The combination of inverters and synchronous motor has many distinct advantages over conventional induction motor drives for applications, e.g., in computer, textile and glass inudstries, requiring precisely constant speed combined with smooth starting capability, constant torque, brushless and relatively noiseless operation. Hysteresis motors idealy meet these drive constraints. Moreover, when used for motor phase control, these motors can be operated on open-loop control schemes, as the motor speed is uniquely determined by the inverter frequency. For inverter-driven hysteresis motors, there exists a further need for more rigorous analysis, particularly of its run-up characteristics.

A series of papers[5-8, 10] have been published on the analysis of hysteresis motors. These analyses are, however, limited to the steady state mode of operation. Although some qualitative representations on asynchronous operation of hysteresis motors have been earlier reported[9-14], there seems to exist a lack of rigorous field analysis of these motors with the notable exception of Teare[3].

F 79 670-1 A paper recommended and approved by the IEEE Rotating Machinery Committee of the IEEE Power Engineering Society for presentation at the IEEE PES Summer Meeting, Vancouver, British Columbia, Canada, July 15-20, 1979. Manuscript submitted January 5, 1979; made available for printing May 1, 1979.

The production of driving torque in hysteresis motors is quite well known[2,4]. The motor when connected to a balanced ac supply, will run up to synchronous speed using hysteresis torque. At standstill, the entire hysteresis energy is lost as heat in the rotor hysteresis ring. During run-up periods, i.e., slip s lying between 1.0 and 0, the torque and output power of an ideal hysteresis motor is given in Fig. 1. At synchronous speed, the hysteresis ring acts the role of a permanent magnet rotor in synchronous motor.

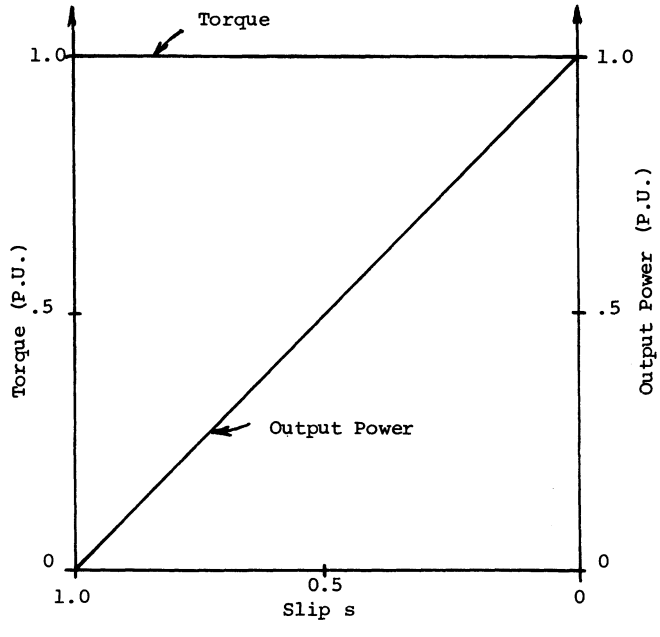

Fig. 1 Torque and Output Power of Ideal Hysteresis Motor as Function of Slip

The scope of this paper is to present a rigorous field analysis of a polyphase hysteresis motor for sub-synchronous speed. Using a stator current sheet model, the field equations of the motor are derived for both the air gap and rotor hysteresis ring regions. Expressions for the air gap power and hysteresis power loss for sub-synchronous speed are obtained.

MATHEMATICAL ANALYSIS

Fig. 2 shows the cross-section of m-phase 2-pole, circumferential-flux hysteresis motor. Field models of the active regions of such motors are shown in Fig. 3. Let x, y, z be the co-ordinate system attached to the stator surface in which the running time is t. Similarly x', y', z' and t' are fixed to the rotor frame such that their transformation becomes:

$$\left.\begin{aligned} x &= x' + (1-s)f\lambda \\ y &= y'-g \\ z &= z' \\ t &= t' \end{aligned}\right\} \quad (1)$$

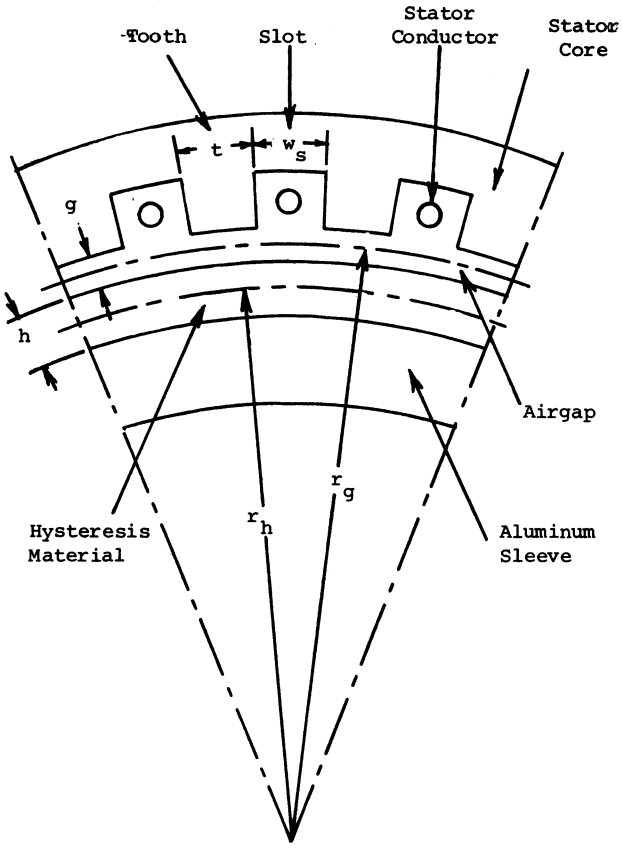

Fig. 2 Cross-Section of Circumferential - Flux Hysteresis Motor

where f = supply frequency and λ = wavelength of travleling spatial current sheet.

REPRESENTATION OF B-H LOOP

The first step in the development of any field model for the hysteresis motor is the approximation of its rotor B-H loop. The analysis is based on small signal, slow-motion conditions so that quasi-static states are applicable. Two principal models[17] namely inclined elliptical[3,9-13], and parallelogram approximation[5] of the B-H loop are employed so as to facilitate the formulation of the machine field equations. Elliptical approximation is relatively easier to handle even though the parallelogram one is sometimes desirable[17]. On the otherhand, the parallelogram approximation leads to a sort of equivalent elliptical one, when the fundamental component of the rotor flux density is concerned.

Based on elliptical approximations, the complex permeability[19-20] of the rotor hysteresis material is given by the relationship $\mu_3 = \mu_{r3}e^{j\beta}$ such that the magnetic field intensity H is denoted as

$$H = Re\{ \hat{H}\, e^{-j\omega t}\} \tag{2}$$

and the corresponding magnetic flux density B is given as

$$B = Re\{ \hat{B}\, e^{-j(\omega t-\beta)} \} \tag{3}$$

The rotor hysteresis material's relative permeability μ_{r3} and hysteresis lag angle β can be easily obtained[18-19] from the given hysteresis loop of the material.

When parallelogram modelling is used, the elliptical equivalent relative permeability μ'_{r3} of the hysteresis ring may be obtained as[5,7]

$$\mu'_{r3} = \frac{\alpha\,\mu_{rp} + \alpha\,\mu_{ro} + \mu_{rp}\mu_{ro}}{\alpha\,\mu_{ro}(\alpha\,\mu_{rp} + \mu_{rp}\mu_{ro})} \tag{4}$$

where $\alpha = \dfrac{g\cdot h}{r_g \cdot r_h}$ and $\mu_{rp} = \dfrac{\mu_{ro}\,\mu_{rs}}{\mu_{ro} - \mu_{rs}}$

μ_{ro} and μ_{rs} are the unsaturated and saturated relative permeabilities respectively, as defined in Fig. 2 of reference 7. Similarly, the modified hysteresis lag angle β' may be obtained directly from equations (19-15) of reference 7. The above modified complex permeability $\mu'_3 = \mu'_{r3}e^{j\beta'}$ is valid for the fundamental component of the rotor flux density.

STATOR CURRENT SHEETS

The technique of using fictitious current sheets on the stator surface is sometimes quite convenient[16]. On the assumption that the field conditions in the air gap just inside and outside of the stator face at $y = -0$ and $+0$ being same, the slot-embedded stator conductors may be replaced by a current sheet of infinitesimal thickness having the same distribution of stator surface current as the slot embedded conductor configurations. The general form of the fundamental current sheet may be written as

$$F = Re\{ \hat{F}\, e^{-j(\omega t - \frac{2\pi}{\lambda} x)} \} \tag{5}$$

For the sake of simplicity, the term Re is dropped.

For the common case of m-phase distributed stator windings having coils with same number of turns and identical geometry, peak value $\hat{F}$ of eqn. (5) can be expressed as[6,16]

$$\hat{F} = \sqrt{2}\, I \frac{mZ}{\lambda} \frac{\sin(\frac{\pi w_s}{\lambda})}{\frac{\pi w_s}{\lambda}} K_d K_p \tag{6}$$

where I = rms stator phase current, Z = number of conductors/phase/pole, w_s = stator slot width, K_d and K_p are the distribution and pitch factors respectively.

The detailed expressions for current sheets for all major types of distributed, concentric, concentrated windings including skewing are given in reference 16.

MOTOR FIELD EQUATIONS

The pertinent Maxwell's equations for the electromagnetic field inside the machine are:

$$\nabla \times H = J + \frac{\partial D}{\partial t} \tag{7}$$

$$\nabla \times E = -\frac{\partial B}{\partial t} \tag{8}$$

$$\nabla \cdot B = 0 \tag{9}$$

where D and E are the electric flux density and electric field intensity respectively.

It is often convenient to make use of the magnetic vector potential A which is defined as

$$\nabla \times A = B \tag{10}$$

In order to define A uniquely, it is necessary to stipulate that[16]

$$\nabla \cdot A = - \mu\varepsilon \frac{\partial A}{\partial t} \tag{11}$$

From equations (8) and 10), one easily obtains

$$E + \frac{\partial A}{\partial t} = - \nabla\phi \tag{12}$$

where ϕ is the scalar potential.

ASSUMPTIONS OF IDEALIZATION

(a) The assumption of neglecting the displacement current is implied in Fig. 3 showing ε=o for the regions 1 and 3

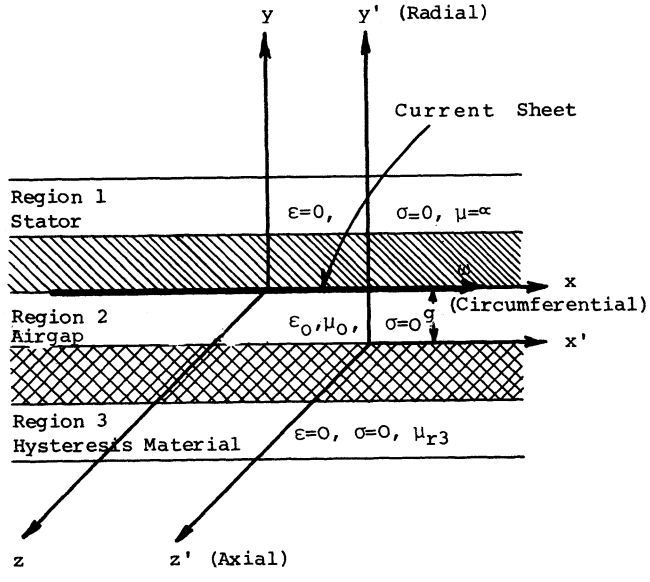

Fig. 3 Machine Field Model Regions

(b) The stator iron is assumed to be non-conducting because of its usual lamination and its permeability is infinite. No current flows in the air gap except that the current sheet is attached to the stator face only.

(c) The rotor hysteresis ring is assumed to be non-conducting in order to neglect the reaction effects of all eddy currents on the main air gap field.

(d) The rotor curvature and end effects are neglected.

On the basis of assumptions (a) - (c), one can obtain the following Laplace's vector and scalar equations.

$$\nabla^2 A = 0 \tag{14}$$

$$\nabla^2 \phi = 0 \tag{15}$$

BOUNDARY CONDITIONS

i) At the stator inner face, the tangential component of H is equal to the surface current density.

ii) The tangential component of H and the radial component of B at the rotor outer surface (y'=0) should be continuous.

iii) The radial component of B at the rotor inner surface (y'=-h) is zero.

In order to overcome the contradiction that the flux lines of gap field due to stator current sheet, which furnishes the excitation of the rotor magnetization, can not penetrate the rotor surface[11], the air gap field is assumed to consist of the superposition of two fields[11,15]. Fig. 4 shows the scalar field patterns in the air gap and rotor regions.

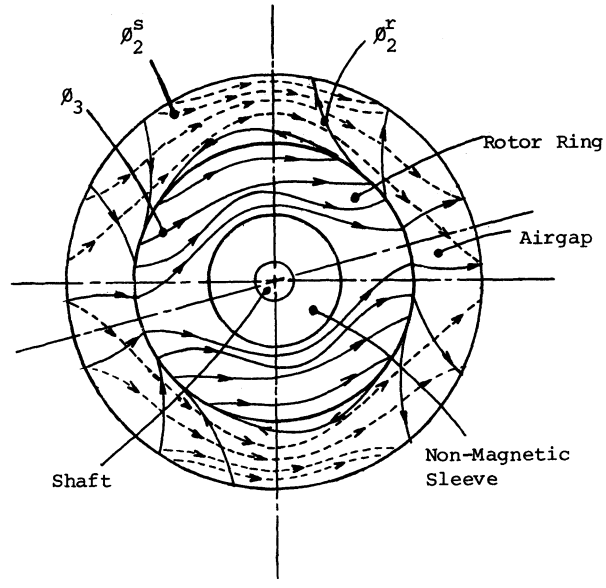

Fig. 4 Field Components Represented by Potential Functions ϕ_2^s , ϕ_2^r and ϕ_3

Let air gap total scalar potential ϕ_2 be given as

$$\phi_2 = \phi_2^s + \phi_2^r \tag{16}$$

where ϕ_2^s represents the air gap scalar potential due to the stator primary current sheet alone and ϕ_2^r represents the contribution of the rotor magnetization to the air gap potential. The corresponding magnetic vector potentials in air gap region are:

$$A_2 = A_2^s + A_2^r \tag{17}$$

For region 2, equations (10) and (12) are redefined as:

$$\nabla x\ (A_2^s + A_2^r) = B_2 = \mu_o H_2 \tag{18}$$

$$E_2 + \frac{\partial}{\partial t}\ (A_2^s + A_2^r) = - \nabla(\phi_2^s + \phi_2^r) \tag{19}$$

Solution of the field equations (14) - (15) in region 2, gives rise to the following expressions of A_2^s, ϕ_2^s, A_2^r and ϕ_2^r for y < o (details are given in the Appendix):

$$A_2^s = \frac{\mu_o \lambda}{2\pi} \hat{F}\, e^{-j(\omega t - \frac{2\pi}{\lambda} x)}\, e^{\frac{2\pi}{\lambda} y} \tag{20}$$

$$\phi_2^s = j\omega \frac{\mu_o \lambda}{2\pi} (z-\ell)\, \hat{F}\, e^{-j(\omega t - \frac{2\pi}{\lambda} x)}\, e^{\frac{2\pi}{\lambda} y} \tag{21}$$

$$A_2^r = C_1 \frac{\mu_o \lambda}{2\pi} \hat{F}\, e^{-j(\omega t - \frac{2\pi}{\lambda} x)} \cosh(\tfrac{2\pi}{\lambda} y) \tag{22}$$

$$\phi_2^r = j\omega \frac{\mu_o \lambda}{2\pi} (z-\ell)\, \hat{F}\, e^{-j(\omega t - \frac{2\pi}{\lambda} x)}$$

$$X \left[C_1 \frac{\sinh(\frac{2\pi}{\lambda} y')}{\sinh(\frac{2\pi}{\lambda} g)} + \frac{\sinh(\frac{2\pi}{\lambda} y)}{\sinh(\frac{2\pi}{\lambda} g)} e^{-j\frac{2\pi}{\lambda} g} \right] \quad (23)$$

where ℓ = axial length

and $$C_1 = \frac{(\mu_{r3} e^{j\beta} - 1) e^{-\frac{2\pi}{\lambda} g}}{\cosh(\frac{2\pi}{\lambda} g) + \mu_{r3} e^{j\beta} \sinh(\frac{2\pi}{\lambda} g)} \quad (24)$$

From equations (18) - (24), one obtains the field components in the region 2 as

$$E_{2x} = \frac{\omega \mu_o (z-\ell) \hat{F}}{\sinh(\frac{2\pi}{\lambda} g)} \left[e^{\frac{2\pi}{\lambda} y} \sinh(\frac{2\pi}{\lambda} g) + C_1 \sinh(\frac{2\pi}{\lambda} y') + e^{-\frac{2\pi}{\lambda} g} \sinh(\frac{2\pi}{\lambda} y) \right] e^{-j(\omega t - \frac{2\pi}{\lambda} x)} \quad (25)$$

$$E_{2y} = -\frac{j\omega \mu_o (z-\ell) \hat{F}}{\sinh(\frac{2\pi}{\lambda} g)} \left[e^{\frac{2\pi}{\lambda}} \sinh(\frac{2\pi}{\lambda} g) + C_1 \cosh(\frac{2\pi}{\lambda} y') + e^{-\frac{2\pi}{\lambda} g} \cosh(\frac{2\pi}{\lambda} y) \right] e^{-j(\omega t - \frac{2\pi}{\lambda} x)} \quad (26)$$

$$E_{2z} = \frac{j\lambda}{2\pi} \frac{\omega \mu_o \hat{F}}{\sinh(\frac{2\pi}{\lambda} g)} \left[C_1 \{\cosh(\frac{2\pi}{\lambda} y) \sinh(\frac{2\pi}{\lambda} g)\} - \sinh(\frac{2\pi}{\lambda} y') - e^{-\frac{2\pi}{\lambda} g} \sinh(\frac{2\pi}{\lambda} y) \right] e^{-j(\omega t - \frac{2\pi}{\lambda} x)} \quad (27)$$

$$H_{2x} = \frac{B_{2x}}{\mu_o} = -\hat{F} \left[e^{\frac{2\pi}{\lambda} y} + C_1 \sinh(\frac{2\pi}{\lambda} y) \right] e^{-j(\omega t - \frac{2\pi}{\lambda} x)} \quad (28)$$

$$H_{2y} = \frac{B_{2y}}{\mu_o} = j\hat{F} \left[e^{\frac{2\pi}{\lambda} y} + C_1 \cosh(\frac{2\pi}{\lambda} y) \right] e^{-j(\omega t - \frac{2\pi}{\lambda} x)} \quad (29)$$

$$H_{2z} = \frac{B_{2z}}{\mu_o} = 0 \quad (30)$$

AVERAGE AIRGAP POWER

The time-average active air gap power flow can be obtained from the Poynting Theorem as $P = \frac{1}{2}$ Re $\{E \cdot H^*\}$. From equations (24) - (30), one gets the expressions of air gap power as:

$$P_{2y} = \left[\frac{\frac{1}{4}(2\pi/\lambda)\omega\mu_o \hat{F}^2 \mu_{r3} \sin\beta}{\cosh^2(\frac{2\pi}{\lambda} g) + \mu_{r3}\cos\beta \sinh(\frac{4\pi}{\lambda} g) + \mu_{r3}^2 \sinh^2(\frac{2\pi}{\lambda} g)} \right] X \left[\frac{\sinh\{(\frac{2\pi}{\lambda})(y'-g)\}}{\sinh(\frac{2\pi}{\lambda} g)} - 1 \right] \quad (31)$$

$$P_{2z} = \left[\frac{-\frac{1}{2}\omega\mu_o (z-\ell) \hat{F}^2 \mu_{r3} \sin\beta}{\cosh^2(\frac{2\pi}{\lambda} g) + \mu_{r3}\cos\beta \sinh(\frac{4\pi}{\lambda} g) + \mu_{r3}^2 \sinh(\frac{2\pi}{\lambda} g)} \right] x \left[\frac{\cosh\{(\frac{2\pi}{\lambda})(y'-g)\}}{\cosh(\frac{2\pi}{\lambda} g)} - 1 \right] \quad (32)$$

Since there is no loss of active power across the air gap, the power received by the rotor becomes:

$$P = -P_{2y} \text{ at } y' = 0 \quad (33)$$

From equations (6), (31) and (33) the expression for rotor input power per unit of its surface area of an m-phase 2-pole motor can be written as

$$P = \frac{(I\, m\, Z\, K_d K_p)^2 \omega \mu_{r3} \mu_o \sin\beta}{2\pi\lambda [\cosh^2(\frac{2\pi}{\lambda} g) + \mu_{r3}\cos\beta \sinh(\frac{4\pi}{\lambda} g) + \mu_{r3}^2 \sinh(\frac{2\pi}{\lambda})]} X \left\{ \frac{\sin(\frac{\pi\omega_s}{\lambda})}{\frac{\pi\omega_s}{\lambda}} \right\}^2 \quad (34)$$

similarly, the solution of equations (14) - (15) in region 3 leads to the following expressions of the field components inside the hysteresis rotor ring

$$E_{3x} = 0 \quad (35)$$

$$E_{3y} = 0 \quad (36)$$

$$E_{3z} = C_2 j s\omega \mu_o \hat{F}\, e^{-j(s\omega t - \frac{2\pi}{\lambda} x' - \frac{2\pi}{\lambda} y')} \quad (37)$$

$$H_{3x} = \frac{B_{3x}}{\mu_{r3} e^{j\beta} \mu_o} = -\frac{C_2 \hat{F}}{\mu_{r3}} e^{-j(s\omega t + \beta - \frac{2\pi}{\lambda} x' - \frac{2\pi}{\lambda} y')} \quad (38)$$

$$H_{3y} = \frac{B_{3y}}{\mu_{r3} e^{j\beta} \mu_o} = j\frac{C_2 \hat{F}}{\mu_{r3}} e^{-j(s\omega t + \beta - \frac{2\pi}{\lambda} x' - \frac{2\pi}{\lambda} y')} \quad (39)$$

$$H_{3z} = 0 \quad (40)$$

where $$C_2 = \frac{\mu_{r3} e^{j\beta} e^{\frac{2\pi}{\lambda} g}}{\cosh(\frac{2\pi}{\lambda} g) + \mu_{r3} e^{j\beta} \sinh(\frac{2\pi}{\lambda} g)} \quad (41)$$

ROTOR AVERAGE POWER LOSS

The time-average power loss in the rotor hysteresis ring can also be obtained from the Poynting Theorem as:

$$P_1 = \frac{1}{2} \text{Re} \{E_{3z} \cdot H_{3x}^*\} \quad (42)$$

Substituting equations (6), (37), (38) and (41) into eqn. (42) at $y' = 0$, the expression for rotor power loss per unit of its surface area of an m-phase 2-pole motor can be written as

$$P_1 = \frac{s(I\,m\,Z\,K_d K_p)^2 \omega \mu_{r3} \mu_o \sin\beta}{2\pi\lambda[\cosh^2(\frac{2\pi}{\lambda}g)+\mu_{r3}\cos\beta\sinh(\frac{4\pi}{\lambda}g)+\mu_{r3}^2\sinh^2(\frac{2\pi}{\lambda}g)]}$$

$$\times \left\{ \frac{\sin(\frac{\pi\omega_s}{\lambda})}{\frac{\pi\omega_s}{\lambda}} \right\}^2 \qquad (43)$$

It is to be noted from equation (34) and (43) that $P_1/P=s$. This is a well known relationship in induction motor theory. The motor output power is thus (1-s) times the rotor input power given in equation (34). Furthermore, equations (25) - (43) provide a deeper inside into the origin of sub-synchronous energy transfer processes in an ideal hysteresis motor, when the slip frequency eddy currents in the hysteresis material are ignored. This analysis is analoguous and consistent to the equivalent circuit models reported earlier[7-8].

EXPERIMENTAL RESULTS

A series of test was carried out on a laboratory motor. The motor has the standard 3-phase 4-pole concentric stator winding and a specially built rotor made of 2mm thin sheets of Oerstit 70 (16% cobalt-steel) hysteresis material. Some of its sample design dimensions and rotor hysteresis material properties are given as follows:

LABORATORY HYSTERESIS MOTOR

Dimensions

Stator inner diameter	130.44mm
Core length	153 mm
Number of poles	4
Number of slots	36
Number of Conductors/slot	76
Conductor Diameter	1 mm
Rotor outer diameter	129.92mm
Length of rotor ring	154 mm
Ring thickness	16.23mm
Air gap length	0.24mm

Rotor Material

Residual flux density	0.8 T
Coercive force	12.5kA/m
Recoil Permeability (μ_{rs})	12.3
Unsaturated Permeability (μ_{ro})	125
Permeability (μ_{r3})	41
Hysteresis lag angle (β)	33.7°
Resistivity	$28\times10^{-6}\Omega$-cm

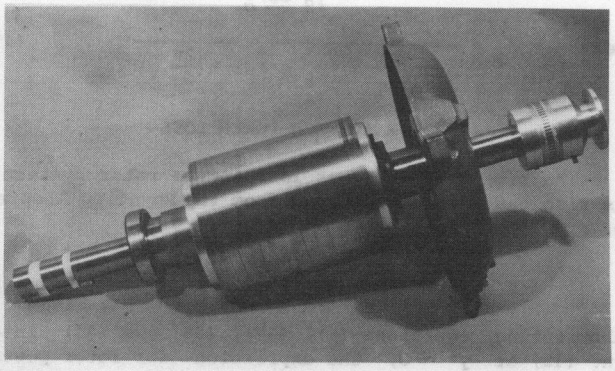

Fig. 5 Experimental Rotor Assembly.

Fig. 5 shows the picture of rotor assembly of the experimental motor. Fig. 6 shows the experimental curves of per unit torque and stator phase current as a function of motor slip. The difference between the measured and theoretically predicted torques in Fig. 6 is due to finite conductivity of the rotor hysteresis material, which is assumed zero for the ideal case.

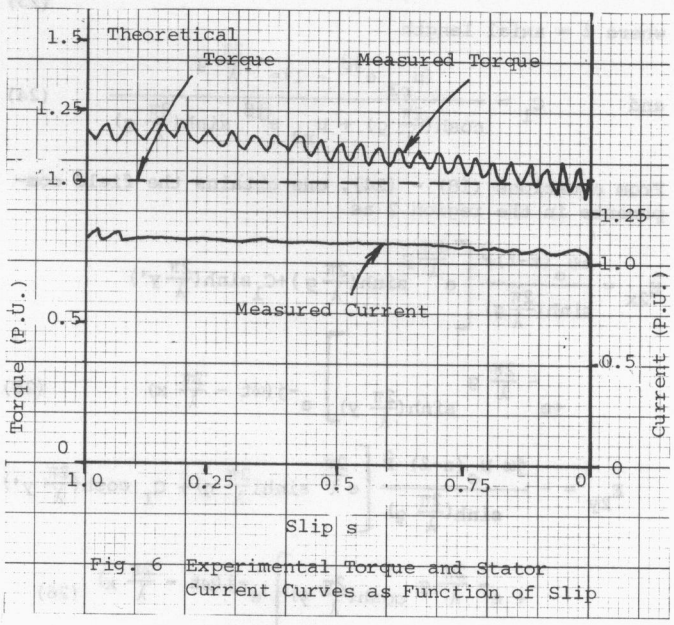

Fig. 6 Experimental Torque and Stator Current Curves as Function of Slip

CONCLUSIONS

A comprehensive theoretical field model of hysteresis motors has been developed. Simplified expressions for air gap power and rotor hysteresis loss material are presented. Non-linearity of the rotor hysteresis material is taken into account by both the inclined elliptical and its equivalent parallelogram models. The field analysis establishes that the reaction effort of magnetization on the air gap field has to be taken into consideration. It also provides a clearer insight into the sub-synchronous torque and hysteresis power loss mechanism inside the rotor. It thus justifies the validity of previously published[7] sub-synchronous equivalent circuit model of the hysteresis element. The agreement between the theoretical and measured results is good enough, considering the complexity of the problem and approximations made in the analysis.

It is hoped that in near future this field analysis approach will be further extended to include the effects of both the fundamental and higher harmonic eddy currents.

ACKNOWLEDGEMENT

The author wishes to acknowledge the encouragement and assistance provided by the General Electric Co., particularly from Drs. T. R. Haller, G. B. Kliman, and T. A. Lipo for this work, while he was a consultant to G.E.

APPENDIX

Fields in Air Gap Region 2

Using equation (7) with no displacement current, the magnetic field at y = 0 becomes[15,13]

$$H_{x(+0)} - H_{x(-0)} = \hat{F}\, e^{-j(\omega t - \frac{2\pi}{\lambda}x)} \qquad (44)$$

where $H_{x(+0)}$ stands for the x-component of the magnetic field just inside the stator face at y = +0, and $H_{x(-0)}$ stands for its counter parts in the air gap just below the stator face at y = -0. Since $\mu_1 = \infty$ for the stator lamination, its magnetic field vanishes and hence eqn. (41) reduced to

$$\lim_{y \to o} H^s_{2x} = - \hat{F}\, e^{-j(\omega t - \frac{2\pi}{\lambda} x)} \tag{45}$$

Using equation (18) for primary magnetic Vector Potential A^s_2 alone, z-component of A^s_2 becomes related to H^s_{2x} by

$$H^s_{2x} = - \frac{1}{\mu_o} \frac{\partial A^s_{2z}}{\partial y} \tag{46}$$

From equations (44) - (45) it is evident, A^s_2 must be coherent in space and synchronous in time with the current sheet excitation. It then satisfied the Laplace's vector equation[15] $\nabla^2 A^s_2 = 0$. Imposing convergence at $y \to - \infty$, one obtains

$$A^s_{2z} = \frac{\mu_o \lambda}{2\pi} \hat{F}\, e^{-j(\omega t - \frac{2\pi}{\lambda} x)}\, e^{\frac{2\pi}{\lambda} y} \quad \text{for } y < o \tag{20a}$$

The corresponding induced electric field is obtained from the above equation as:

$$E^s_{2z} = - \frac{\partial A^s_{2z}}{\partial t} = j\omega \frac{\mu_o \lambda}{2\pi} \hat{F} e^{-j(\omega t - \frac{2\pi}{\lambda} x)} \quad \text{for } y = 0 \tag{47}$$

From equation (12) it is also evident that this electric field given in eqn. (47) must be offset by an additional component forming part of the primary scalar potential ϕ^s_2. The latter satisfies the Laplace's scalar equation[15] $\nabla^2 \phi^s_2 = 0$. Stipulating again convergence for $y \to - \infty$ and imposing the boundary condition

$$\lim_{y \to o} (- \frac{\partial \phi^s_2}{\partial z}) = - j\omega (\frac{\mu_o \lambda}{2\pi}) \hat{F}\, e^{-j(\omega t - \frac{2\pi}{\lambda} x)} \tag{48}$$

one obtains eqn. (21) for ϕ^s_2.

The contribution on the air gap field by the rotor magnetization, represented by A^r_2 and ϕ^r_2 is confined to the air gap region only. This rotor contributing field, although primarily caused by the stator current sheet, is not required to allow for the excitation at the stator surface y = o. Thus A^r_2 is coherent and synchronous with A^s_2. The z-component of A^r_2 is expressed as

$$A^r_{2z} = C_1 \frac{\mu_o \lambda}{2\pi} \hat{F} e^{-j(\omega t - \frac{2\pi}{\lambda} x)} \cosh(\frac{2\pi}{\lambda} y) \quad \text{for } y < o \tag{22a}$$

It satisfies the vector Laplace's equation[15] $\nabla^2 A^r_2 = 0$. Imposing the current sheet at the stator face y = 0 stipulates the boundary condition as

$$\lim_{y \to o} H^r_{2x} = \lim (- \frac{1}{\mu_o} \frac{\partial A^r_{2z}}{\partial y}) = 0 \tag{49}$$

While the solution given by equation (22a) satisfies the boundary condition of eqn. (49), it leads to an induced electric field component as

$$E^r_{2z} = C_1 j\omega \frac{\mu_o \lambda}{2\pi} \hat{F}\, e^{-j(\omega t - \frac{2\pi}{\lambda} x)} \quad \text{for } y = 0 \tag{50}$$

It is evident from equation (12) that the above electric field E^r_{2z} of eqn. (50) must be offset by an additional component forming part of scalar field ϕ^r_2. In view of continuity of field at the rotor interface,

$$\phi^s_2 + \phi^r_2 = 0 \qquad \text{at } y' = 0 \tag{51}$$

Similarly the scalar potential ϕ^r_2 must also satisfy the scalar Laplace's equation $\nabla^2 \phi^r_2 = 0$, which gives rise to its expression as given in equation (23).

The expressions for magnetic vector and scalar potentials of eqns. (20) - (23) when referred to the rotor frame of co-ordinate systems (x', y', z', t') becomes

$$A^{s'}_2 = \frac{\mu_o \lambda}{2\pi} \hat{F}\, e^{-j(s\omega t' - \frac{2\pi}{\lambda} x')} e^{\frac{2\pi}{\lambda} y'} \tag{52}$$

$$\phi^{s'}_2 = js\omega \frac{\mu_o \lambda (z' - \ell)}{2\pi} \hat{F} e^{-j(s\omega t' - \frac{2\pi}{\lambda} x')} e^{\frac{2\pi}{\lambda} y'} \tag{53}$$

$$A^{r'}_2 = C_1 \frac{\mu_o \lambda}{2\pi} \hat{F} e^{j(s\omega t' - \frac{2\pi}{\lambda} x')} \cosh\{\frac{2\pi}{\lambda}(y' - g)\} \tag{54}$$

$$\phi^{r'}_2 = js\omega \frac{\mu_o \lambda}{2\pi} (z' - \ell)\, \hat{F}\, e^{-j(s\omega t' - \frac{2\pi}{\lambda} x')}$$

$$\times \left[C_1 \frac{\sinh(\frac{2\pi}{\lambda} y')}{\sinh(\frac{2\pi}{\lambda} g)} + \frac{\sinh\{\frac{2\pi}{\lambda}(y' - g)\}}{\sinh(\frac{2\pi}{\lambda} g)} e^{-j \frac{2\pi}{\lambda} g} \right] \tag{55}$$

FIELDS IN ROTOR REGION 3

The resultant electric field from equations (47) and (50) has only a z'- component. Continuity of this field across the rotor surface at y' = 0 implies that the rotor magnetic vector potential A_3 has only z- component throughout the rotor region 3 for $-\infty < y' < -g$. The requirements of coherence, synchronism and convergence yield that

$$A_{3z'} = C_2 \frac{\mu_o \lambda}{2\pi} \hat{F} e^{-j(s\omega t - \frac{2\pi}{\lambda} x')}\, e^{\frac{2\pi}{\lambda} y'} \tag{56}$$

The electric field $E_{3z'}$ inside the rotor becomes

$$E_{3z'} = - \frac{\partial A_{3z'}}{\partial t'} \tag{57}$$

While the magnetic flux density has x' and y' components from eqn. (10) as:

$$\left. \begin{aligned} B_{3x'} &= - \frac{\partial A_{3z'}}{\partial y'} \\ B_{3y'} &= \frac{\partial A_{3z'}}{\partial x'} \end{aligned} \right\} \tag{58}$$

By virtue of the assumed potential functions, the requirement of continuity for the x'-directed electric field component is automatically satisfied at y' = 0.

Applying the continuity requirement for z'-directed electric field and x'-directed magnetic field at the rotor interface y ' = 0, one gets the following set of equations

$$-\frac{\partial}{\partial t'}\left(A^{s'}_{2z'}+A^{r'}_{2z'}\right)-\frac{\partial}{\partial z'}\left(\phi^{s'}_{2}+\phi^{r'}_{2}\right)=-\frac{\partial A_{3z'}}{\partial t'} \qquad (59)$$

and

$$-\frac{1}{\mu_o}\frac{\partial}{\partial y'}\left(A^{s'}_{2z'}+A^{r'}_{2z'}\right)=-\frac{1}{\mu_{r3}e^{j\beta}\mu_o}\frac{\partial A_{3z'}}{\partial y'} \qquad (60)$$

Using equations (52) - (56) and (59) - (60), one eventually gets the expressions for the constants C_1 and C_2 as given in equations (24) and (41) respectively.

Continuity of y-directed component of the magnetic flux density at y' = 0 is automatically ensured. As for the radial discontinuity of the conservative electric field at y' = 0, it does not give rise to any charges in view of assumed zero value of ε.

REFERENCES

[1] M.A. Rahman and S.D. Gowda, "Representative Bibliography on Hysteresis Motors", IEEE Paper No. A79 071-2, IEEE PES Winter Meeting, New York, Feb. 04 - Feb. 09, 1979.

[2] D. Robertson, "Rotor hysteresis in polyphase induction motor", The Electrician, Vol. 68, 1911, pp. 12-14.

[3] B.R. Tears, "Theory of hysteresis motor torque", AIEE Transactions, Vol. 59, 1940, pp. 907-912.

[4] H. C. Roters, "The hysteresis motor, advances which permit economical fractional hp ratings", AIEE Transactions, Vol. 66, 1947, pp 1419-1430.

[5] M.A. Copeland and G.R. Slemon, "An analysis of the hysteresis motor, II-The circumferential flux machine", IEEE Transactions, Vol. Pas-83, June 1964, pp 619-625.

[6] M. A. Rahman, M. A. Copeland and G. R. Slemon, "An Analysis of the hysteresis motor, III Parasitic Losses", IEEE Transactions, Vol. Pas-88, No. 6, June 1969, pp. 954-961.

[7] M.A. Rahman, "Analytical models for polyphase hysteresis motor", IEEE Transactions, Vol. PAS-92, No. 1, January/February 1973, pp 237-242.

[8] G. R. Slemon, R. D. Jackson and M.A. Rahman, "Performance Predictions for Large Hysteresis Motors" IEEE Transactions Vol. Pas-96, Nov-Dec 1977, pp 1915-1919.

[9] D. O'Kelly, "Equivalent circuits for single Phase induction and hysteresis motors", IEEE Transaction, Vol. PAS-90, No. 1, 1971, pp 2790288.

[10] G. Wakui and Y. Kusakari, "Synchronous Pull-out torque of hysteresis motor", JIEE, Japan, Vol. 85, 1965, pp 31-41.

[11] S.D.T. Robertson and S.Z.G. Zaky, "Analysis of hysteresis machines part I", IEEE Transactions, Vol. PAS-88, April 1969, pp 474-483.

[12] S. Miyairi and T. Kataoka, "Analysis of hysteresis motors, considering eddy current effects", JIEE Japan, Vol. 86, No. 6, 1966, pp. 67-77.

[13] D. Schieber, "Asynchronous performance of hysteresis Motor", J. Franklin Inst., Vol. 299, No. 6, 1975, pp 433-47.

[14] J. Perard and M. Poloujadoff, "Asynchronous performance of Hysteresis Motors under Unbalanced Condition", Electric Machines and Electromachanics, An International Quarterley, Vol. 1, No. 4, July-Sept. 1977, pp 377-389.

[15] F. Ollendorff, "Über Unipolare Induktion", Archiv für Elektrotechnik, Vol. 44, 1959, pp 80-94.

[16] R.M. Saunders, "Electromechanical Energy Conversion in double cylindrical structures", IEEE Transactions, Vol. PAS-82, 1963, pp 631-638.

[17] M.A. Rahman, "Performance of higher rating polyphase hysteresis motor", Proceedings International Conference on Electrical Machines", Part I, City University London, 2-6th Sept. 1974, pp-c-5, 1-10.

[18] H. Liebsch, "Läufer werkstoffe für hysteresmotoren", Elektrie, Heft 7, 1962, pp 230-233.

[19] K.A. Macfaden, "Vector Permeability", Journal IEE, Vol. 94, Part 3, 1947, pp 407-414.

[20] D. O'Kelly, "Theory and performance of solid rotor induction and Hysteresis Machines", Proc. IEE, Vol. 123, No. 5, 1976, pp 421-428.

M. Azizur Rahman (S'66, M'68, SM'73) was born in Sanatahar Bangladesh, on January 9, 1941. He received the B.Sc. Engg. degree in electrical engineering from the Bangladesh University of Engineering and Technology, Dacca, the M.A. Sc. degree from the University of Toronto, and the Ph.D. degree from Carleton University, Ottowa, Canada, in 1962, 1965 and 1968, respectively.

In 1962 he joined the Department of Electrical Engineering, Bangladesh University of Engineering and Technology, as a staff member and worked as Associate Professor till May 1974. From 1963-1964 he was a Consultant with the Dacca Electric Supply. In 1968 he joined the Engineering Laboratory, Canadian General Electric Company, Peterborough, Ontario, Canada as a Research Scientist. In 1973 he was a visiting Research Fellow at the Technische Hogeschool Eindhoven, Netherlands. In 1974-1975 he was a Nuffield Fellow at the Imperial College, London, England. He was a visiting professor at University of Toronto working on large hysteresis motors during the summer of 1975. During 1975-1976 he was at Teshmont Consultants Ltd. Winnipeg, Manitoba and part-time staff at the University of Manitoba. Since September 1976, he is an Associate Professor at the Memorial University of Newfoundland, Canada and acts as Consultant to outside firms including General Electric Corporate Research and Development, Schenectady, N. Y. His current interests are in machines, Power systems and Power Electronics.

Dr. Rahman is a registered professional engineer in the provinces of Ontario and Newfoundland. He is a member of I.E., Bangladesh.

Discussion

Gordon R. Slemon (University of Toronto, Toronto, Canada): Dr. Rahman is to be complimented on extending his previous analysis to give insight into the sub-synchronous operation of a hysteresis motor. It would be interesting to know what effect the neglect of air-gap curvature has on this analysis. In small machines, where the change in radius may be significant, would the use of a cylindrical co-ordinate system have been justified?

Figure 6 shows an experimental torque which appears to have high ripple content. One of the advantages normally claimed for hysteresis machines is the constancy of the torque during the speed-up process. Did these ripples actually occur, or did they arise from vibrations in the measurement system?

An extension of this paper would be to include the effects of eddy currents during the speed-up of the process. Does the author feel that a simple superposition of eddy current and hysteresis effects is appropriate, or does a more elaborate theory have to be developed to include these effects?

Manuscript received July 31, 1979.

J. Perard and **M. Poloujadoff** (Institut National Polytechnique de Grenoble, Grenoble, France): We welcome the paper of our colleague Professor Rahman, and we are glad to answer to his call for discussion.

We have three comments:

First, we have had great difficulties when representing the hysteresis loops by parallelograms or ellipses. Indeed, small differences of interpretation, introduced during the passage from real cycles to "equivalent" cycles, have led us to differences in the predicted torque which were commonly of the order of ± 5%, and have attained 20%. That is the reason why we have tried to characterize the hysteretic properties of the rotor material by integrals which were precisely defined from the actual, complete, cycle [A], [B]. This cannot be done if it is not accepted to make some errors on the evaluation of the field.

Second, it is unfortunate that we have no time to discuss the fundamentals of the field computation, because of the delays which are given to send a discussion. We hope to give precisions on this point later on.

Third, we believe that Professor Rahman's experimental work could be of great use for future developments, if it was fully published. As a matter of fact, his method leads to predict a torque which is independent of speed; therefore, it is necessary to know the variation of this torque as a function of primary current. The knowledge of the active and reactive power at the input terminals would give another precious method to check the validity of theoretical studies.

As far as the data are concerned, several hysteresis cycles should be given instead of μ_{rs}, μ_{r3}, μ_{r0}, β, $H_c(max)$, and $B_r(max)$, which, as we have said earlier, define a poor characterization of the material.

Knowledge of the winding is also of interest. Indeed, it is known [Fig. 6 of ref. B] that the torques of an hysteresis machine are not the same during motor operation and d-c brake operation, even if the primary mmf is the same; the discrepancies can be attributed to the mmf distribution harmonics, which are determined by the nature of the winding [C].

We would like also to know what is the air-gap indicated by the author: is it the mechanical clearance, or the air-gap computed from some Carter coefficient? Changes in the definition of the air-gap may also introduce noticeable variations in the results.

We hope that such precisions can be given, and we compliment Professor Rahman for his contribution.

REFERENCES

[A] J. Perard, M. Poloujadoff: Determination du champ magnétique et du couple dans un moteur hystérésis polyphasé à moyeu amagnétique. C. R. Acad. Sc. Paris, t.275, Série B, pp. 239-242 (1972).

[B] J. Perard, M. Poloujadoff: Etude des moteurs à hystérésis polyphasés à bague moyennement épaisse. Revue Générale de l'Electricité, t.83 n°2, pp. 71-75 (1974).

[C] J. Perard, M. Poloujadoff: Fonctionnement des moteurs à hystérésis en régime asynchrone déséquilibré. Revue E, vol. III n°10, pp. 265-269 (1974).

Manuscript received July 9, 1979.

M. A. Rahman: The author wishes to thank the discussors for their stimulating comments. Professor Slemon is quite correct about his concern on the ripples in Fig. 6. These ripples on the torque curve were indeed picked up due to vibration of the measurement systems. As regards the effect of neglecting the airgap curvature, it is more of a convenience to facilitate the solutions of equations (14) - (15) in cartesian co-ordinates. It is an approximation but it does not appreciably affect the result of the analysis qualitatively. The author fully agrees with Professor Slemon that more elaborate works have to be carried out to include the eddy current effects in the total analysis of the hysteresis motors, the results of which will be reported in a future paper.

As regards the questions of Dr. Perard and Professor Poloujadoff, the following additional design data on the stator are: The stator windings are 3-phase, Y-connected and standard concentric type. The slot opening is 2.5 mm. The slot shape is standard type with a depth of 25.3 mm, top-radius of 2.85 mm and bottom-radius of 4.4 mm. The tooth rim is 0.5 mm thick. The airgap clearance given in the text is a mechanical one. However, for computational purposes, modified airgap using Carter's coefficient was taken care of.

In reply to the question on MMF-harmonis the computed values were not adjusted for any parasitic losses due to both MMF and Flux-harmonics. However, some detailed analysis on the effects of these harmonics are given in reference [6]. The author fully agrees with Professor Poloujadoff that the predicted terminal performance results of the hysteresis motor are critically dependent on the types of B-H loop models used. The author is pursuing the modelling of B-H characterization by digital methods using modified Frölich approach[D], Neél's method[A,14], along with parallelogram methods[E]. The results of comparative methods will be reported in the near future. A typical B-H loop cycle of the experimental hysteresis ring material, Oerstit-70, is given in Fig. A.

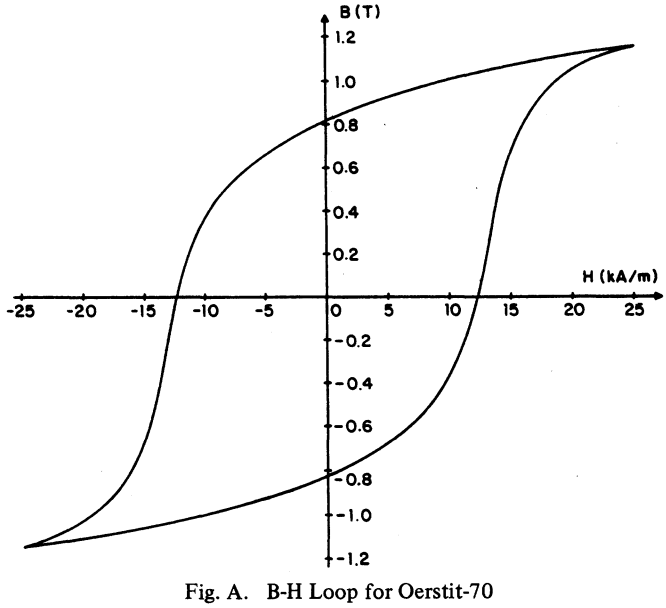

Fig. A. B-H Loop for Oerstit-70

REFERENCES

[D] J. S. Everatt, "Computer Simulation of Non-linear inductor with hysteresis", Electron letter, No. 6, 1970, pp. 833-4.

[E] R. D. Jackson, "Digital Simulation of the Hysteresis Motor", Proc. I.E.E., Vol. 120, No. 12, 1973, pp. 1533-37.

Manuscript received November 6, 1979.